Mon. Not. R. Astron. Soc. **325,** 995–1001 (2001)

Constraints on the nuclear emission of the Circinus galaxy: the torus

M. Ruiz,[1★] A. Efstathiou,[2] D. M. Alexander[3] and J. Hough[1]

[1]*Department of Physical Sciences, University of Hertfordshire, Hatfield, Herts AL10 9AB*
[2]*Astrophysics Group, Imperial College, Blackett Laboratory, Prince Consort Road, London SW7 2BZ*
[3]*Penn State University, Astronomy and Astrophysics, Davey Laboratory, University Park, PA 16802, USA*

Accepted 2001 February 20. Received 2001 February 12; in original form 2000 July 21

ABSTRACT

In the context of the unified model of Seyfert galaxies, we use observations from the literature and a radiative transfer model to investigate the near-IR to mm emission produced by the presumed torus in the Circinus galaxy, from 2 μm to 1.3 mm. From the infrared SED modelling, we find that the total luminosity (L_{IR}) in this wavelength range consists of similar contributions from the torus and starburst with a ratio of nuclear luminosity to starburst luminosity (L_{NUC}/L_{SB}) ~ 0.8.

By using a similar torus model to that of NGC 1068, *but without the conical dust*, we find an upper limit to the outer torus radius of ~12 pc with a best fit of ~2 pc. The upper limit torus size estimated from the radiative transfer modelling is consistent with the 16-pc torus radius estimated from near-IR imaging polarimetry of Circinus.

Key words: radiative transfer – galaxies: active – galaxies: individual: Circinus – galaxies: nuclei – infrared: galaxies.

1 INTRODUCTION

Observational evidence for obscuring material in the centres of active galactic nuclei (AGN) is now abundant. Obscuration is observed in the form of molecules and dust, present in the centres of these galaxies on scales that vary from a fraction of a parsec to tens and even hundreds of parsecs (Greenhill et al. 1996; Gallimore et al. 1997; Siebenmorgen et al. 1997; Malkan et al. 1998). It is believed that the obscuring material takes the form of a dusty 'torus' which blocks and absorbs part of the radiation from the active nucleus. These dusty tori play an essential role in unified theories of Seyfert galaxies and strongly support the unification models.

The unified model for Seyfert galaxies proposes that all types of Seyfert galaxy are fundamentally the same, but the presence of the dusty torus obscures the nucleus, including the broad-line emission region in many systems. In this picture the classification of Seyfert 1 or 2 depends on the inclination angle of the torus to our line of sight (e.g. Antonucci & Miller 1985; Antonucci 1993). Strong support for this model has come from X-ray observations, showing that Seyfert 2 galaxies are Compton thick, i.e. the nuclear radiation is absorbed by matter with column densities $>10^{24}\,\mathrm{cm}^{-2}$ (Lawrence & Elvis 1982; Maiolino et al. 1998a).

Direct imaging of the presumed torus is technically demanding due to its (predicted) small size (e.g. Efstathiou, Hough & Young 1995, hereafter EHY95; Granato, Danese & Franceschini 1997; Alexander et al. 1999). The most convincing direct evidence for a Seyfert torus comes from observations of the HCN molecule (Jackson et al. 1993), which traces dense molecular gas, and near-IR imaging polarimetry (Young et al. 1996), both of NGC 1068. These images show a large nuclear structure of ~200 pc in extent, approximately perpendicular to the [O III]5007 emission cone and radio lobe emission. Indirect support for tori comes from ground-based narrow-band imaging (e.g. Wilson & Tsvetanov 1994), high-resolution *HST* imaging (e.g. Capetti, Axon & Macchetto 1997; Falcke, Wilson & Simpson 1998) and imaging-polarimetry (e.g. Packham et al. 1997; Lumsden et al. 1999; Tadhunter et al. 1999; Ruiz et al. 2000) which have shown a number of objects with nuclear cone-like structures, presumably collimated by the torus.

The origin of the infrared continuum in a number of Seyfert 2 galaxies is clearly thermal as indicated by silicate features such as the broad absorption at 10 μm (Roche et al. 1991) and the various emission features from polycyclic aromatic hydrocarbons (PAHs), e.g. 3.3, 6.2 and 11.3 μm, which are normally associated with the presence of hot stars in a starburst environment. Dust grains, distributed in a toroidal geometry surrounding the central black hole and accretion disc, are believed to be responsible for the absorption of radiation from the central source and re-radiation of energy into longer wavelengths giving rise to the observed 'IR bump' longwards of 1 μm and peaking at mid-IR wavelengths (Rowan-Robinson & Crawford 1989). The resultant radiation spectrum is dependent on the distribution of dust grain temperatures (≤2000 K) and optical depth. Two additional components can add to the IR spectra of active galaxies (Rowan-Robinson & Crawford 1989): galactic diffuse emission from large dust grains heated by the interstellar radiation field in the galactic

★E-mail: mili@star.herts.ac.uk

disc (cirrus, $T_{\rm large\ grains} \leq 40$ K) and a starburst component peaking at about 60 μm.

Thus, a radiative transfer model which takes into account dust grain features within a true toroidal configuration and starburst environment is needed to reproduce correctly the near-IR to mm spectral energy distribution (SED) of the Circinus galaxy.

Here, we present a model for the IR continuum emission of the Circinus galaxy which successfully fits the observations from 2 μm to mm wavelengths. We constrain the size and flux of the dusty AGN torus and estimate the contribution of the starburst emission to total IR emission. Section 2 presents the data compilation and Sections 3 and 4 present the model and the fitting procedure. Section 5 discusses the model and its implications, and conclusions are summarized in Section 6.

2 THE DATA

The continuum and PAH data points have been compiled from a variety of sources in the literature and are presented in Table 1. The data sources will be described below. There is a large range of sizes in the observational apertures, from arcsec to arcminute beamsizes, equivalent to physical sizes of < 5 pc and > 200 pc (for Circinus, 1 arcsec corresponds to 20 pc); whenever possible, data from the smallest available aperture were used to minimize the contribution from galactic disc emission.

In the near-IR, below 2 μm, the stellar contribution is quite significant, and to study the nuclear emission, the starlight contribution has to be subtracted from the integrated flux. The data point at 2.2 μm shown in Table 1 corresponds to the deconvolved non-stellar measurement as presented by Maiolino et al. (1998b) and derived from a 0.15-arcsec aperture. This measure will set a limit on the size of the nuclear non-stellar source (see Section 2.1).

In the mid-IR, between 3 and 20 μm, the continuum data points at 3.8 and 4.8 μm are provided by Siebenmorgen et al. (1997) who carried out speckle interferometry in the L'(3.8 μm) and M(4.8 μm) bands with a 0.3-arcsec aperture. The speckle observations are insensitive to larger scale components, e.g. starlight, and predict more directly the nuclear non-stellar contribution (see Section 4). Other continuum data points over this wavelength range are from the *ISO*–SWS spectrum presented in Sturm et al. (2000).

Line information for the PAH features at 3.28, 6.2, 7.7, 8.6 and 11.3 μm were directly measured from the *ISO*–SWS spectrum in Sturm et al. (2000). The reported values in Table 1 correspond to the peak of these emission lines. *ISO* apertures are large enough ($\sim$24 arcsec^2) to contain much of the circumnuclear star forming regions as well as the nuclear emission. The *ISO* spectrum shows that the region between 5 and 12 μm is dominated by PAH features, characteristic of star formation activity (see Fig. 1), and it is remarkably similar to those of pure starburst galaxies also observed by ISOPHOT (Siebenmorgen, Krügel & Zota 1999).

The spectrum corresponding to the Si absorption feature centred at 9.7 μm is shown in more detail in Fig. 1. It was provided by P. Roche and published by Roche et al. (1991). This spectrum was taken with the UCL spectrometer and used an aperture of 4.3 arcsec. For comparison also shown in Fig. 1 is the mid-IR *ISO*–SWS spectrum of Circinus taken with the much larger aperture of 14×20 arcsec^2 (Sturm et al. 2000).

The N(10.3 μm) band continuum data point is also provided by Siebenmorgen et al. (1997) and measured through a 1.3-arcsec slit. It is interesting to note that a larger aperture measurement at 10.3 μm by Moorwood & Glass (1984) with a 5-arcsec aperture is very similar to the smaller aperture data of Siebenmorgen et al. (1997). This is a good indication of the compact nature of the central source at this wavelength. The continuum data points at 20, 30 and 40 μm were taken from the *ISO*–SWS spectrum (Sturm et al. 2000). The *ISO* SWS spectrum at 25 μm agrees within 20 per cent of the *IRAS* flux.

The far-IR continuum observations were collected from the *IRAS* large-aperture observations (90 arcsec) at 12, 25, 60 and

Table 1. IR–mm data points.[a]

λ (μm)	Flux (Jy)	Beamsize	Reference[b]
2.2[c]	0.022	0.15 arcsec	1
3.0	1.1	14×20 arcsec^2	2
3.28[d]	2.0	14×20 arcsec^2	2
3.8[b]	0.777	0.3 arcsec	6
4.8[b]	1.832	0.3 arcsec	6
6.2[c]	8.5	14×20 arcsec^2	2
7.7[c]	20.0	14×20 arcsec^2	2
8.6[c]	10.0	14×20 arcsec^2	2
10.3[b]	6.32	1.5 arcsec	6
11.3[c]	20.0	14×20 arcsec^2	2
12	19	90 arcsec	4
20	45	14×20 arcsec^2	2
30	100	14×20 arcsec^2	2
40	200	14×20 arcsec^2	2
25	65	90 arcsec	4
60	280	90 arcsec	4
100	340	90 arcsec	4
150[e]	<150	40 arcsec	5
1300	0.248	23 arcsec	6

[a] Collected from the literature. Data for the 7–13 μm range are shown in Fig. 1.
[b] References: (1) Maiolino et al. (1998b); (2) Sturm et al. (2000); (3) Moorwood & Glass (1984); (4) *IRAS*, Moshir et al. (1992); (5) Ghosh et al. (1992); (6) Siebenmorgen et al. (1997).
[c] Nuclear measurement.
[d] PAH feature peak.
[e] 5σ upper limit.

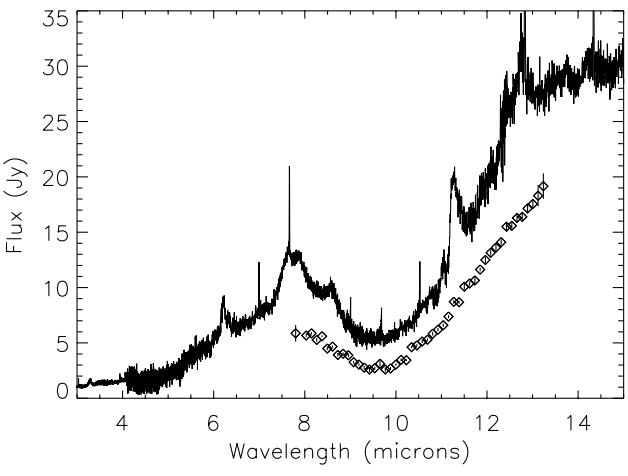

Figure 1. Circinus mid-IR spectrum. The solid line corresponds to the Circinus *ISO*–SWS (Sturm et al. 2000) spectrum and square open points correspond to the Roche et al. data. The *ISO* spectrum is dominated by emission features from PAHs as the *ISO*–SWS spectrum was taken with a large aperture (14×20 arcsec^2). Note the lack of these emission features in the Roche et al. data (aperture $\sim$4.2 arcsec).

100 μm as reported by Moshir et al. (1992). The continuum data point at 150 μm was taken from the analysis by Ghosh et al. (1992) which corresponds to an aperture of 40 arcsec. This measurement is only a 5σ upper limit as Circinus was not detected at this wavelength.

At millimetre wavelengths, Circinus has been detected at 1.3 mm with an aperture of 23 arcsec as reported by Siebenmorgen et al. (1997). Maps of the millimetre continuum emission show Circinus as an unresolved source.

Clearly, the large-aperture observations are contaminated with light from various emission sources, particularly from the extended galactic disc; thus, special care is needed when fitting the large-aperture data points to the individual emission components in the radiative transfer model (see next section).

2.1 Constraints from observational data

In the *K* band (2.2 μm), the source is clearly unresolved in a 0.3-arcsec aperture (6 pc on source). By deconvolving the nuclear *K*-band surface brightness radial distribution with a stellar profile and a nuclear point spread function (PSF), Maiolino et al. (1998b) set a constraint on the size of the nuclear non-stellar source of $<$1.5 pc. Similarly, at 3.8 and 4.8 μm the source is also observed to be unresolved at 0.7-arcsec resolution and is possibly $<$0.3 arcsec in size, setting upper limits of 6 pc (Siebenmorgen et al. 1997). Clearly, at wavelengths $\leq$5 μm most of the emission comes from a central source with a size $\leq$6 pc. This size scale almost certainly corresponds to the inner radius of the proposed dusty torus, as the near-IR emission is most likely to result from hot dust grains ($T \leq 1300$ K) heated by the intense radiation from the non-stellar central source. *Thus, in our model, the near-IR data points at $<$5 μm are assumed to be totally dominated by the emission from the torus component.*

Observations at 10 μm reveal that the central source size is possibly resolved with a size of 26 pc whilst at 20 μm it is unresolved and $<$30 pc in size (Siebenmorgen et al. 1997). As mentioned in the previous section, the emission detected with the larger aperture of Moorwood & Glass (1984) at 10 μm does not seem very different from that of the smaller aperture by Siebenmorgen et al. (1997). At wavelengths larger than 20 μm, the IR emission most likely results from a more extended region, and there is possibly a significant contribution from the inner circumnuclear starburst ($\sim$40 pc in radius).

The spatial resolution analysis at 60, 100 and 150 μm by Ghosh et al. (1992) reveals a deconvolved size of Circinus of 40 arcsec at 50 μm. However, at these longer wavelengths, the resolution is too poor to put useful constraints on the size of the emitting source.

The spectrum corresponding to the Si feature at 9.7 μm (Fig. 1) was taken with an on-source equivalent aperture of $\sim$80 pc (Roche et al. 1991). The detection of a number of CO stellar absorption features in a 4.4×6.6 arcsec^2 aperture gives strong evidence for circumnuclear star formation in a region few tens of parsecs from the nucleus (Oliva et al. 1994; Maiolino et al. 1998b), thus the Si feature cannot be solely modelled by dust self-absorption from the torus component, but a starburst contribution will have to be included when fitting this feature with the SED model.

The long-wavelength data points and PAH features (*IRAS* and *ISO* data), which correspond to large-aperture observations (see Table 1), are hence dominated by the larger scale starburst emission observed in the circumnuclear ring at $\sim$200 pc from the nucleus. Thus, the data points corresponding to *IRAS* and *ISO* data are fitted with a starburst component.

3 THE GENERAL INFRARED MODEL

The model used is the radiative transfer model of Efstathiou and co-workers as described in detail in Efstathiou & Rowan-Robinson (1995, hereafter ER95), EHY95 and Efstathiou, Rowan-Robinson & Siebenmorgen (2000, hereafter ERS00). This radiative transfer model has been successful in fitting the IR continuum of NGC 1068 (EHY95) and Centaurus A (Cen A) (Alexander et al. 1999). The proposed model for the SED of the Circinus galaxy is a combination of the following two components described below.

3.1 Torus

As concluded in ER95, the most likely geometry for the obscuring material in the centre of AGNs is that of a 'tapered disc'. Other proposed geometries for the torus are 'flared discs' (Efstathiou & Rowan-Robinson 1990, hereafter ER90; Granato & Danese 1994) or cylinders (Pier & Krolik 1992, 1993; Taniguchi & Murayama 1998). However, the shape of the IR continuum spectrum of type 1 and type 2 objects, the appearance of the 10-μm silicate features and the statistics of the two types of Seyfert galaxies give strong support for a tapered disc geometry (see ER95 for detailed discussion). Indeed, there is further confirmation of the validity of the tapered disc geometry to represent the nuclear emission of tori in AGNs realistically. This comes from the fitting of IR data to a sample of Seyfert galaxies with the EHY95 models of their fig. 3. They have been successfully used to fit nuclear (non-stellar) near-IR observations for a sample of Sy1s and Sy2s (Alonso-Herrero et al. 2001) showing that the near-IR nuclear emission from Seyfert galaxies can be fitted with the tapered disc geometry tori of EHY95. We therefore assume this geometry for the Circinus torus. As demonstrated in ER90, the orientation of the plane of the system to the line of sight is a very important parameter when fitting the observed spectra, since only a small difference in this inclination parameter, θ_V, produces a significant variation in the emergent spectrum. Another important parameter that determines the shape of the IR continuum is the half-opening angle of the torus, Θ. In general, these parameters are not known for most objects, but fortunately, we have a good idea of their values from spectropolarimetry (Alexander et al. 2000) and IR-imaging polarimetry of Circinus (Ruiz et al. 2000) which gives $\theta_V \sim 40^\circ$ (measured from the axis of the torus to the line of sight) and $\Theta \sim 45^\circ$. Although the emission-line cones observed in Circinus and many other AGNs offer a measure of the opening angle of the torus, it is common to find that the conical emission 'opens up' as light travels and scatters in the circumnuclear medium. Thus, we should keep in mind that Θ can be smaller than that derived from emission-line cones (see Section 4).

Other parameters that will affect the shape of the emergent SED spectrum are: the ratio of the inner and outer radii (r_1/r_2), the ratio of the height to the outer radius (h/r_2), the equatorial optical depth ($^{eq}A_{UV}$), the dust sublimation temperature (T_1) and the radial dependence of the density distribution $r^{-\beta}$. To take into account the effects of dust in the nuclear regions of Circinus, we assume that there is an additional extinction (i.e. in addition to that produced by the torus). Marconi et al. (1994) found $A_V \geq 20$ mag towards the nucleus. This limit follows from the fact that we can see the nucleus at 1.25 μm but are unable to do so at 7000 Å, thus they only set a lower limit for the nuclear extinction. However, we find that $A_V = 25$ mag is required to fit the near-IR data successfully. This value is also close to that found by Moorwood & Glass (1984) from the depth of silicate feature at 9.7 μm, and is

also consistent with that estimated by Maiolino et al. (1998b). Based on *H*- and *K*-band observations, they set a minimum extinction $A_V > 12$ mag toward the nucleus of Circinus. From their images, it is clear that this obscuration is caused by the large amounts of dust as seen in their $H-K$ colour map and it is due to the presence of a nuclear gas bar. Their estimated A_V, however, is only a lower limit and we expect a larger value since the extinction is most likely to be due to an inhomogeneous distribution of dust, gas and stars. The parameters assumed for the torus model are listed in Table 2.

3.2 Starburst

The radiative transfer models of starburst galaxies are described in detail in ERS00. The models consider a starburst galaxy as an ensemble of optically thick giant molecular clouds centrally illuminated by recently formed stars. The stellar population is determined according to the Bruzual & Charlot (1993) stellar population synthesis models. The grain model used is that of Siebenmorgen & Krügel (1992) and the emission of transiently heated dust grains is calculated according to their method. In the models, the effects of multiple scattering are taken into account. The models relate the observed properties of a galaxy to its age and star formation history. These models have successfully matched the observational characteristics of M82 and other starburst galaxies (ERS). Various populations of dust particles are considered:

(i) Mathis, Rumpl & Nordsieck (1977) – these are large particles with a size distribution of classical grains;

(ii) small graphite grains, to account for the extinction bump at around 2175 Å (Draine 1989);

(iii) PAH molecules, to explain the near-IR and mid-IR emission bands.

To take into account the effects of dust in the starburst regions of Circinus, we impose on the starburst emission an extinction of $A_V = 5$ mag, as measured from narrow emission line ratios (Oliva et al. 1994). This is lower than the additional extinction assumed to the nucleus (Section 3.1), as the starburst is expected to be outside the circumnuclear molecular bar.

Table 2. Model parameters.

Best-fitting torus parameters	
system inclination[a], θ_V (°)	50
cone opening half-angle, Θ (°)	30
$^{eq}A_{UV}$ (mag)	1000
$^{eq}A_V$ (mag)	200
$^{los}A_V$ (mag)	83[b]
T_1(K)[c]	1000
β[d]	1
additional A_V[e] (mag)	25
Best-fitting starburst parameters	
Starburst e-folding time	10 Myr
Starburst age	26 Myr
τ_V, initial GMC optical depth	50
A_V in ISM (mag)	5
A_V through Galactic disc (mag)	1.5

[a] Measured from the plane of the torus to the line of sight.
[b] $^{eq}A_V$ corrected for the inclination of the torus to the line of sight.
[c] Dust sublimation temperature at torus inner radius.
[d] Value determined as discussed in EHY95.
[e] Due to circumnuclear bar.

4 MODEL FITTING

As described in Section 3, the data points will be fitted to the SED model components according to the observational constraints described in Section 2.1. The critical wavelength range is likely to be where the torus and starburst components are equally important, that is in the 10–30 μm region. Here, the strong absorption feature is indicative of the presence of dust in the form of silicates which are likely to be present in a dusty environment such as the torus; however, the observational beam for this data is large enough to cover a region which also includes star formation. Thus, contributions from both the torus and starburst components are important in this wavelength range. On the other hand, given that the near-IR points are to be modelled by the torus alone (see Section 2.1), this sets a strong constraint on the number of possible models to be tested for the torus. Similarly, in the long-wavelength range and large-aperture data points which include the PAH features, the starburst component dominates, and only a number of starburst models can be applied. Thus, the overall fitting procedure is much better constrained and the number of free parameters reduced once the short- and long-wavelength ranges are considered.

The torus input parameters that reproduce the near-IR points are listed in Table 2. The best fits were obtained with a cone half-opening angle of 30°, the same as the best fit obtained for the NGC 1068 torus model (EHY95). One important difference with the NGC 1068 model is that there is no requirement to include a contribution from hot dust in the torus cone. Indeed, if this is included, then it is very difficult to obtain a fit to the near-IR data points. The starburst parameters that reproduce the PAH features and large-scale emission successfully are also listed in Table 2. Table 3 presents the derived geometrical characteristics for the best-fitting torus in Circinus. In Fig. 2 we show the best model for the SED of the Circinus galaxy which is the addition of the torus and starburst models. Note that the solid line (representing the total emission from the galaxy) exceeds the mid-infrared data of Roche et al. (1991). This is not surprising as the starburst which contributes about half of the emission is more extended than the 4-arcsec aperture of Roche et al. (1991). Thus, the final SED for the 10-μm absorption feature should not fit the 9.7-μm data of Roche et al. 1991 (Fig. 1).

Unfortunately, there is a serious lack of small-aperture (nuclear) data in the range of 30–60 μm. As a consequence, we are unable to rule out tori up to ~12 pc although increasing the torus outer radius further would produce far too much 30–60 μm flux. Future observations in this critical wavelength range will put extra constraints on the torus model, and the torus size would be determined more accurately.

It is interesting to note in Fig. 2 the overall larger contribution to the total IR emission of the starburst compared with the torus component. This is indicated by the ratio of the nuclear

Table 3. Torus characteristics.

r_1/r_2	0.05
h/r_2	0.5
Inner radius (r_1, pc)	0.12
Outer radius (r_2, pc)	2.4
Height (h, pc)	1.2

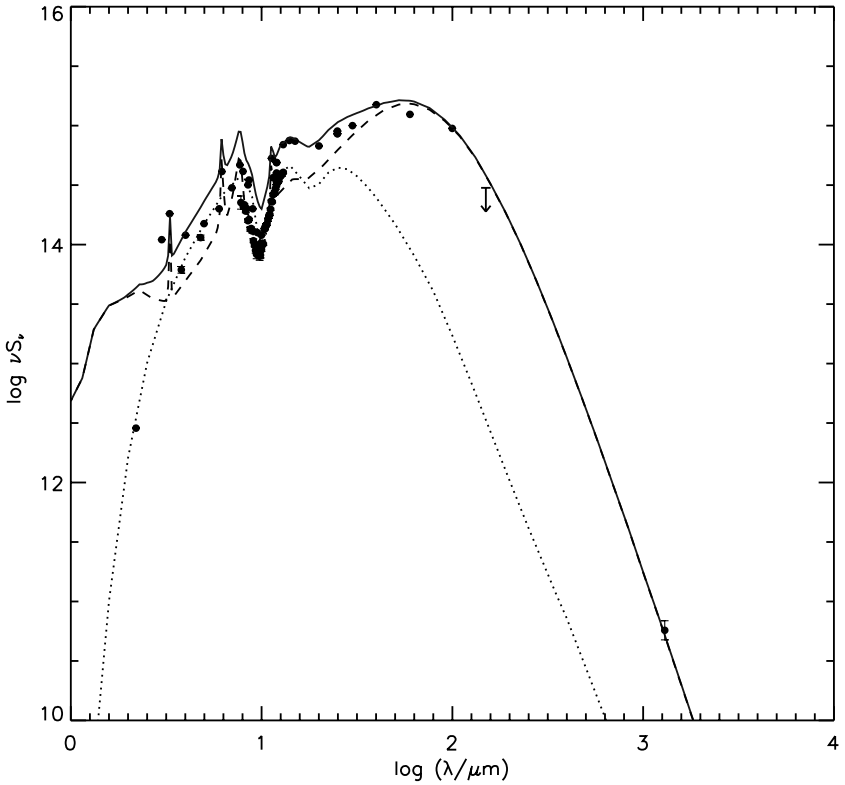

Figure 2. IR SED for the Circinus galaxy. The SED is fitted with a starburst and a torus model. Dark circles are the data points from Table 1 and Fig. 1. Units for νS_ν are 10^{-26} W m^{-2}. The dotted line corresponds to the torus component, the dashed line is the starburst component and the solid line represents the total fit. The model parameters assumed for the torus and starburst are given in Table 2.

luminosity (torus component) to the starburst luminosity (starburst component) ($L_{\rm NUC}/L_{\rm SB}$) $\sim$ 0.8 (see next section).

5 DISCUSSION

Our SED model shows that, overall, the starburst contribution to the total IR luminosity, $L_{\rm IR}$, slightly dominates over the torus contribution. A direct result of this is the relatively small size of the torus in Circinus, with a best fit of $\sim$2 pc for the outer radius, comparable to the torus outer radius of 1.8 pc modelled for Cen A (Alexander et al. 1999) but significantly smaller than the $\sim$90 pc torus for NGC 1068 (EHY95; Young et al. 1996). This result is smaller than that calculated from the near-IR imaging polarimetry modelling of Ruiz et al. (2000) which suggests that the torus is approximately 16 pc in radius, although consistent with our upper limit of $\sim$12 pc.

So far, by using the radiative transfer models of ER95 we have been able to model the size of the torus outer radius for three objects: NGC 1068 (EHY95), Cen A (Alexander et al. 1999) and Circinus (this work). Although the statistics are small, it is interesting to note that all three AGN can be modelled with tori of very similar parameters. This suggests that whatever the mechanism that forms these tori in an AGN–starburst environment, it is such that the size of the tori scales with the luminosity of the central source but the rest of the torus parameters (Table 2) are scale invariant. For example, the hard X-ray continuum, which is considered to be a good indicator of the central source strength, indicates that the Circinus galaxy is a relatively low-luminosity AGN (Matt et al. 1996), while NGC 1068 is $\sim$100 times more powerful (Turner et al. 1997), with a torus radius $\sim$100 pc. The predicted torus radii scale as $L^{1/2}$, reflecting the fact that both objects can be fitted with very similar radiative transfer models.

Of great debate regarding the nature of the Circinus galaxy is the ratio of the AGN to starburst emission ($L_{\rm NUC}/L_{\rm SB}$), that is, the relative contribution of the torus and starburst components to the total $L_{\rm IR}$. Previous predictions from IR modelling differ widely. As already mentioned, Rowan-Robinson & Crawford (1989) found a 20 per cent contribution of the nuclear component to the total $L_{\rm IR(10-100\,\mu m)}$ and $L_{\rm NUC}/L_{\rm SB} \sim 0.3$ while this work suggests a $L_{\rm NUC}/L_{\rm SB}$ of 0.8. On the other hand, from the Brα luminosity, Moorwood et al. (1996) estimate that this ratio is perhaps as high as 9. Our result is in very good agreement with that suggested by Maiolino et al. (1998b) who estimate from *K*-band observations a $L_{\rm NUC}/L_{\rm SB}$ ratio of 0.9 for the region < 200 pc. Similarly, we agree with the ratio derived from the inferred ionizing continuum required to produce the highly ionized IR lines, suggesting a ratio closer to 1 (Moorwood et al. 1996). We believe that the differences are caused by a number of pitfalls. For example, Rowan-Robinson & Crawford (1989) modelled the far-IR (10–100 μm) *IRAS* data with a three-component model, a starburst, a Seyfert and a disc cirrus-like component. This model assumed a spherically symmetric dust distribution with a power-law density distribution, $n(r) \sim r^{-\beta}$. In this model, radiation from the polar regions of the torus is absorbed by the spherical dust cloud. Thus, this model will naturally underestimate the nuclear component, as their low $L_{\rm NUC}/L_{\rm SB}$ ratio shows. However, there is now ample observational evidence that favours the existence of axially symmetric distributions of dust (ER90; ER95). On the other hand, the large $L_{\rm NUC}/L_{\rm SB}$ ratio derived by Moorwood et al. (1996) suggests a strongly dominant AGN over the starburst. This was derived from

the comparison of near-IR recombination lines in Circinus and M82; from a Brγ map (Moorwood & Oliva 1994), they assume that 50 per cent of the recombination lines are produced in the nucleus of Circinus. However, this is likely to be an overestimation of the strength of Brγ in the nucleus since, more recently, a more accurate measurement of the Circinus nuclear recombination lines (Maiolino et al. 1998b) has shown that only ~10 per cent of the total recombination-line flux is produced in the nucleus of Circinus. Thus, assuming the standard relation between Brα flux and total IR luminosity in starburst galaxies, we can determine the contribution of the starburst to $L_{\rm IR}$. We find $L_{\rm SB} \sim 8.5 \times 10^9\,{\rm L}_\odot$, so $L_{\rm NUC}/L_{\rm SB} \sim 1.2$ for an AGN luminosity of $10^{10}\,{\rm L}_\odot$. This is in good agreement with the ratio we find from the SED modelling.

Radio observations suggest that at these wavelengths, the starburst emission is the dominant component (Forbes & Norris 1998) and Circinus would certainly be classified as a starburst galaxy based purely on radio emission. Indeed, it is interesting to note that the FIR–radio correlation established by Helou, Soifer & Rowan-Robinson (1985), which is followed by normal spiral and starburst galaxies, is closely followed by the Circinus galaxy, confirming the Forbes & Norris result. However, it is almost certain that this correlation is the result of large-scale star formation activity unrelated to the Seyfert activity which generates both the synchrotron radio emission and the thermal FIR emission. Given that the Circinus galaxy has strong star formation activity on small and large scales, it is not surprising that this galaxy follows the FIR–radio correlation. Radio observations at arcsec resolution cannot easily distinguish between Seyfert and starburst activity. The radio emissions from both starburst regions and Seyfert nuclei have similar spectra and morphology, and the steep spectrum of even the compact cores seen in VLA maps of Seyferts suggests that they might contain a significant nuclear starburst component (Norris et al. 1992). On the other hand, long-baseline radio interferometry is sensitive only to compact, high-brightness objects and is an ideal tool to discriminate over the two spatial scales. Unfortunately no radio interferometry is available for the Circinus galaxy and we cannot clearly determine the nature of the central source from present radio data.

Nevertheless, there is a clear large variation in the predicted $L_{\rm NUC}/L_{\rm SB}$ ratios for Circinus, from starburst-dominated at FIR wavelengths, to AGN-dominated in the near- and mid-IR. Indeed, NGC 1068, the prototypical Seyfert 2 galaxy, shows a similar behaviour. The mid-IR(5–16 μm) spectrum of NGC 1068 is ~85–95 per cent dominated by the AGN, and $L_{\rm NUC}/L_{\rm SB} \sim 3$. In the FIR, however, where extended emission dominates, the nucleus does not contribute more than 25 per cent to the total IR flux at 450 μm (Le Floc'h et al. 2001). Clearly, determination of $L_{\rm NUC}/L_{\rm SB}$ is strongly dependent on the spectral region where it is calculated.

Our SED modelling has the advantages over other predictions of having a more complete model for the SED, including the emission of PAH features, and a more realistic torus model. Additionally we have used a large set of recently published data, from NIR to mm wavelengths. More importantly, we pay special attention to the fit of data points from the various aperture sizes which give important constraints to the size of the emitting source. The undoubted composite nature of the Circinus galaxy is shown in our IR SED model which predicts a galaxy dominated by the AGN torus at near- and mid-IR wavelengths while at far-IR to mm wavelengths the starburst activity is dominant.

6 CONCLUSIONS

We can summarize our results as follows.

(i) The case of the Circinus galaxy provides strong support for the dusty torus model of active galaxies which further supports the unification scheme: that is, thick dusty tori with a tapered disc geometry surrounding the central engine.

(ii) Our best fit for the outer radius of the torus in Circinus is ~2 pc, but a radius as large as 12 pc cannot be ruled out.

(iii) We confirm the composite nature of the Circinus galaxy, which is dominated by the AGN torus emission in the near-IR but largely dominated by starburst phenomena in the far-IR and mm wavelengths. The $L_{\rm IR}$ is slightly dominated by the starburst emission and the ratio $L_{\rm NUC}/L_{\rm SB} \sim 0.8$.

ACKNOWLEDGMENTS

We thank P. Roche for providing the mid-IR spectrum of Circinus and D. Sturm for providing the *ISO*–SWS spectrum. We thank A. Alonso-Herrero and the anonymous referee for useful comments. MR and AE thank PPARC for support through a postdoctoral assistantship. DMA thanks the TMR network (FMRX-CT96-0068) for support through a postdoctoral grant while working on this project. This research has made use of the NASA/IPAC Extragalactic Database (NED), which is operated by the Jet Propulsion Laboratory, California Institute of Technology, under contract with NASA.

REFERENCES

Alexander D. M., Efstathiou A., Hough J. H., Aitken D. K., Lutz D., Roche P. F., Sturm E., 1999, MNRAS, 310, 78
Alexander D. M., Heisler C. A., Young S., Bailey J. A., Hough J. H., Lumsden S. L., 2000, MNRAS, 313, 815
Alonso-Herrero A., Quillen A. C., Simpson C., Efstathiou A., Ward M. J., 2001, AJ, 121, 1369
Antonucci R., 1993, ARA&A, 31, 473
Antonucci R., Miller J., 1985, ApJ, 297, 621
Bruzual G., Charlot S., 1993, ApJ, 405, 538
Capetti A., Axon D., Macchetto F. D., 1997, ApJ, 487, 560
Draine B. T., 1989, in Allamandola L., Tielens A. G. G., eds, Proc. IAU Symp. 135, Interstellar Dust. Kluwer, Dordrecht, p. 313
Efstathiou A., Rowan-Robinson M., 1990, MNRAS, 273, 649 (ER90)
Efstathiou A., Rowan-Robinson M., 1995, MNRAS, 273, 649 (ER95)
Efstathiou A., Hough J. H., Young S., 1995, MNRAS, 277, 1134 (EHY95)
Efstathiou A., Rowan-Robinson M., Siebenmorgen R., 2000, MNRAS, 313, 734 (ERS00)
Falcke H., Wilson A. S., Simpson C., 1998, ApJ, 502, 1998
Forbes D. A., Norris R. P., 1998, MNRAS, 300, 757
Gallimore J. F., Baum S. A., O'Dea C. P., 1997, Nat, 388, 743
Ghosh S. K., Bisht R. S., Iyengar K. V. K., Rengarajan T. N., Tandon S. N., Verma R. P., 1992, ApJ, 391, 111
Granato G. L., Danese L., 1994, MNRAS, 268, 235
Granato G. L., Danese L., Franceschini A., 1997, ApJ, 486, 147
Greenhill L. J., Gwinn C. R., Antonucci R., Barvainis R., 1996, ApJ, 472, L21
Helou G., Soifer B. T., Rowan-Robinson M., 1985, ApJ, 298, L7
Jackson J. M., Paglione T. A. D., Ishizuki S., Nguyen Q. R., 1993, ApJ, 418, L13
Lawrence A., Elvis M., 1982, ApJ, 256, 410
Le Floc'h E., Mirabel I. F., Laurent O., Charmandaris V., Gallais P., Sauvage M., Vigroux L., Cesarsky C., 2001, astro-ph/0101038
Lumsden S. L., Moore T. J. T., Smith C., Fujiyoshi T., Bland-Hawthorn J., Ward M. J., 1999, MNRAS, 303, 209

Maiolino R., Salvati M., Bassani L., Dadina M., Della Ceca R., Matt G., Risaliti G., Zamorani G., 1998a, A&A, 338, 781
Maiolino R., Krabbe A., Thatte N., Genzel R., 1998b, ApJ, 493, 650
Malkan M. A., Gorjian V., Tam R., 1998, ApJS, 117, 25
Marconi A., Moorwood A. F. M., Origlia L., Oliva E., 1994, Messenger, 78, 20
Mathis J. S., Rumpl W., Nordsieck K. H., 1977, ApJ, 217, 425
Matt G. et al., 1996, A&A, 315, L109
Moorwood A. F. M., Glass I. S., 1984, A&A, 135, 281
Moorwood A. F. M., Oliva E., 1994, Infrared Phys. Tech., 35, 349
Moorwood A. F. M., Lutz D., Oliva E., Marconi A., Netzer H., Genzel R., Sturm E., de Graauw T., 1996, A&A, 315, L109
Moshir M., Kopman G., Conrow T. A. O., 1992, in Moshir M., Kopman G., Conrow T. A. O., eds, *IRAS* Faint Source Survey: Explanatory Supplement version 2. Infrared Processing and Analysis Center, California Institute of Technology, Pasadena
Norris R. P., Roy A. L., Allen D. A., Kesteven M. J., Troup E. R., Reynolds J. E., 1992, in Filippenko A., ed., ASP Conf. Ser. Vol. 31, Relationships Between Active Galactic Nuclei and Starburst Galaxies. Astron. Soc. Pac., San Francisco, p. 71
Oliva E., Salvati M., Moorwood A. F. M., Marconi A., 1994, A&A, 288, 457
Packham C., Young S., Hough J. H., Axon D. J., Bailey J. A., 1997, MNRAS, 288, 375
Pier E., Krolik J., 1992, ApJ, 401, 99
Pier E., Krolik J., 1993, ApJ, 418, 673
Roche P. F., Aitken D. K., Smith C. H., Ward M. J., 1991, MNRAS, 248, 606
Rowan-Robinson M., Crawford J., 1989, MNRAS, 238, 523
Ruiz M., Alexander D. M., Young S., Hough J. H., Lumsden S., Heisler C., 2000, MNRAS, 316, 49
Siebenmorgen R., Krügel E., 1992, A&A, 259, 614
Siebenmorgen R., Moorwood A. F. M., Freudling W., Käufl H. U., 1997, A&A, 325, 450
Siebenmorgen R., Krügel E., Zota V., 1999, A&A, 351, 140
Sturm E., Lutz D., Tran D., Feuchtgruber H., Genzel R., Kunze D., Moorwood A. F. M., Thornley M. D., 2000, A&A, 358, 481
Tadhunter C., Packham C., Axon D. J., Jackson N. J., Hough J. H., Robinson A., Young S., Sparks W., 1999, ApJ, 512, L91
Taniguchi Y., Murayama T., 1998, ApJ, 501, L25
Turner T. J., George I. M., Nandra K., Mushotzky R. F., 1997, ApJ, 488, 164
Wilson A. S., Tsvetanov Z. I., 1994, AJ, 107, 1227
Young S., Packham C., Hough J. H., Efstathiou A., 1996, MNRAS, 283, L1

This paper has been typeset from a TEX/LATEX file prepared by the author.